ACS OMEGA

http://pubs.acs.org/journal/acsodf

Article

Role and Mechanism of Exosome-Derived Long Noncoding RNA HOTAIR in Lung Cancer

Lanlan Chen, Shenhui Huang, Jincheng Huang, Qiujuan Chen, and Qihong Zhuang*

Cite This: *ACS Omega* 2021, 6, 17217−17227

Read Online

ACCESS | Metrics & More | Article Recommendations

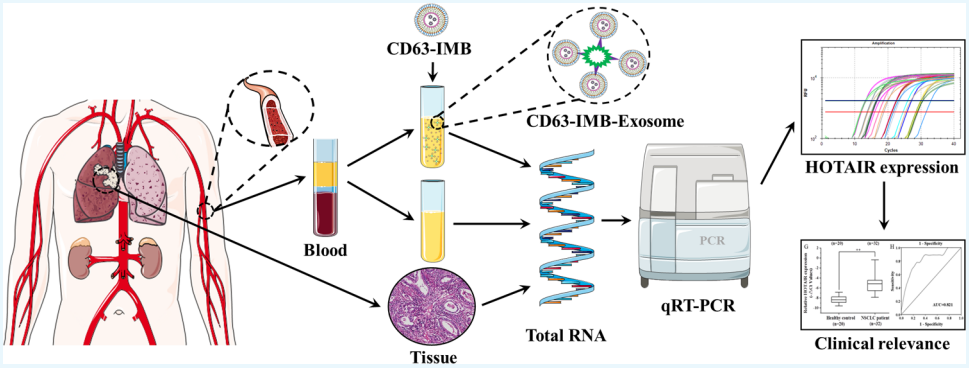

ABSTRACT: Background and purpose: HOX transcript antisense RNA (HOTAIR) is a long noncoding RNA (lncRNA) that promotes tumor growth and metastasis. Exosomes can mediate intracellular communication in cancer by transferring active molecules. However, the role and mechanism of HOTAIR in nonsmall cell lung cancer (NSCLC) are still unclear. This study mainly explores the role and mechanism of exosome-derived HOTAIR in NSCLC. Methods: after the material characterization of the CD63 immune lipid magnetic bead (CD63-IMB), the exosomes in serum of NSCLC patients were captured through CD63-IMB for the corresponding biological characterization. Real-time quantitative reverse transcription PCR (qRT-PCR) was performed to detect the expression level of HOTAIR in tumor tissues, serum, and serum exosome from NSCLC patients. Subsequently, exosome secreted by NCI-H1975 cells with highly expressed HOTAIR was selected to treat low-expression A549 cells and HOTAIR knockdown on NCI-H1975 cells. In this way, action mechanisms of HOTAIR can be investigated by means of qRT-PCR, colony formation assays, and flow cytometry. Results: exosomes can be isolated by CD63-IMB, and taken up by cells effectively; the qRT-PCR results demonstrate that HOTAIR expressions are significantly upregulated in tumor tissues, serums, and exosomes isolated from serums of NSCLC patients. Clinicopathological correlation analysis shows that the upregulation of HOTAIR is closely associated with lymphatic metastasis and tumor node metastasis (TNM) staging ($P < 0.05$). HOTAIR expressions show a significant increase in A549 cells treated with exosomes derived from NCI-H1975 cells, signifying that both proliferation and migration of A549 cells are promoted, and HOTAIR depletion could inhibit the proliferation and migration of lung cancer cells. Conclusions: HOTAIR is highly expressed in tumor tissues, serums, and serum exosomes of NSCLC patients and its expression has a significant correlation with lymphatic metastasis and TNM staging. Moreover, the exosome may promote NSCLC proliferation and migration through HOTAIR transportation. Therefore, exosome-derived HOTAIR is expected to be a new molecular marker for NSCLC diagnosis, and exosomal transmission of HOTAIR may provide a new approach to NSCLC diagnosis.

1. INTRODUCTION

Lung cancer is one of the top malignant tumors with high incidence and mortality in the world,[1] of which nonsmall cell lung cancer (NSCLC)(NSCLC) accounts for 80−85%.[2] If lung cancer was diagnosed at an early stage, aggressive surgery has to be performed to excise tumor lesions to significantly improve the patient's long-term prognosis and quality of life.[3] However, early detection techniques, including chest radiography, sputum cytology, and widely applied low-dose CT scan, did not provide patients with a significant survival advantages. NSCLC patients may miss their optimal surgery time due to the following reasons.[4] First, no symptoms of discomfort occurred from early to late stages. Second, when confirmed, most patients were in the late lung cancer stage. According to statistical data, a 5 year

Received: February 19, 2021
Accepted: June 11, 2021
Published: June 29, 2021

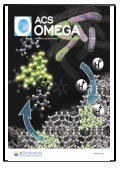

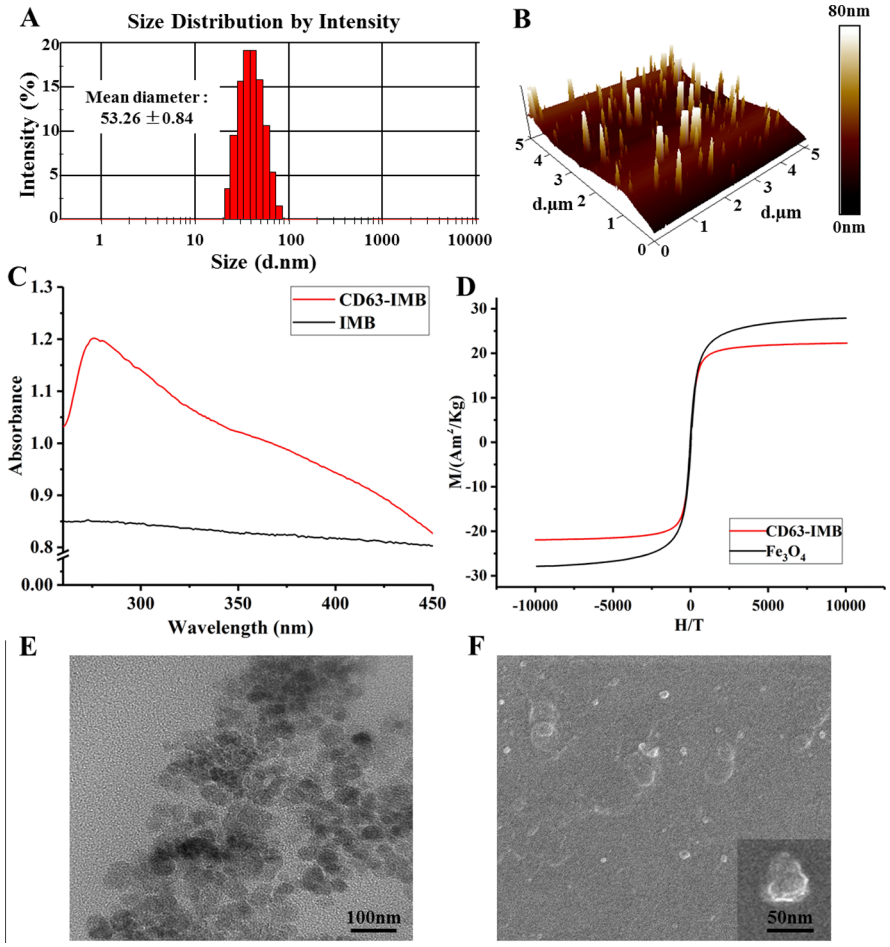

Figure 1. CD63-IMB characterization testing results: (A) size distribution of CD63-IMB; (B) CD63-IMB observed under an atomic force microscope; (C) ultraviolet absorption of CD63-IMB; (D) magnetic crystallinity of CD63-IMB; (E) TEM observation results; and (F) SEM observation results.

survival rate of patients with lung cancer is only close to 15.9%.[5−8] Based on this, it is both urgent and challenging for researchers to seek potential molecular diagnostic biomarkers that are reliable and valuable.

Recently, long noncoding RNAs (lncRNAs) longer than 200 base sequences are found, which can play various important roles during occurrence and progression of tumors.[9,10] LncRNAs are capable of regulating gene expressions, affecting biological functions of tumor cells through pretranscription and post-transcription. HOTAIR is the first lncRNA reported to be associated with malignant tumors, and HOTAIR can influence tumor occurrence through cell proliferation, migration, invasion, and apoptosis.[11−13] Reversely transcribed from 12q13 Human HOXC genes,[14] HOTAIR is closely related to cell proliferation, invasion, and recurrence of small-cell NSCLC.[15] Studies show that HOTAIR may be a reliable and effective novel potential marker, which may contribute to NSCLC diagnosis, progression evaluation, and survival time prediction. Exosomes are small membranous vesicles of the endocytic origin.[16] Increasing evidence suggests that exosomes could promote tumor initiation, development, and progression.[17] Previous studies have shown that exosomes contain proteins, miRNAs, and lncRNAs.[18,19] LncRNAs could be protected by exosomes from degradation in the circulation[20] and could be useful for diagnosing cancer at the early stage.[21]

In this study, for the first time, HOTAIR in serum exosomes is used for evaluating whether HOTAIR can be used as a biomarker for NSCLC diagnosis. Specifically, exosome expressions in serums are tested by qRT-PCR to find their relationship with clinical pathology. Therefore, by studying the mechanism of HOTAIR on the cell proliferation and migration of NSCLC and revealing the biological functions of HOTAIR from exosomes in NSCLC, this study provides a new molecular target for the diagnosis of NSCLC.

2. RESULTS AND DISCUSSION

2.1. CD63-IMB Characterization Testing. During nanoparticle tracking analysis (NTA), Brownian motion posterior to CD63-IMB exosome is observed and the average particle size and the polydispersity index of CD63-IMB are calculated to be 53.26 ± 0.84 nm and 0.198, respectively. The range of the particle size distribution is from 23.35 to 86.24 nm. As shown in Figure 1A, the prepared CD63-IMB is rather stable and uniformly distributed. Under an atomic force microscope, CD63-IMB is observed to be spherical with diverse sizes, and no agglomerations are found, which signifies that CD63 immune lipid magnetic beads are stable in solutions (Figure 1B). It can be found in the ultraviolet−visible spectrum that the CD63 antibody has an absorption peak at 260−280 nm, while IMB has no absorption peak, indicating that the absorption peak appears after the CD63 antibody and IMB are combined to form

https://doi.org/10.1021/acsomega.1c00905
ACS Omega 2021, 6, 17217−17227

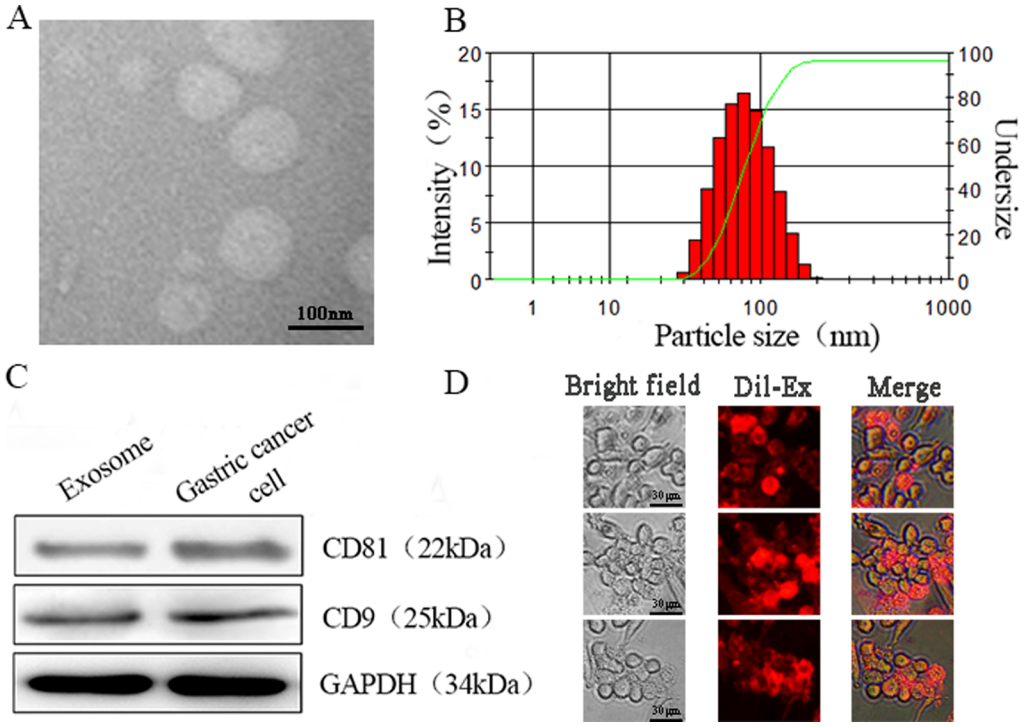

Figure 2. Identification of exosomes: (A) TEM results of exosomes; (B) particle size distribution of exosomes; (C) Western blot results of exosomes; and (D) expression of exosome marker (Dil).

magnetic microspheres, so the surface of the IMB is connected to the CD63 antibody. The curve of IMB draws increasingly near to that of the CD63 antibody as presented in Figure 1C. According to magnetization curves, it is clear that no hysteresis curves are generated at room temperature by Fe_3O_4 magnetic particles or CD63-IMB; however, both of them show superparamagnetism. Saturation magnetization of Fe_3O_4 magnetic particles or CD63-IMB turns out to be, respectively, 28.23 and 22.18 Am^2/kg by intensity (Figure 1D). Based on this, it is proved that the Fe_3O_4 magnetic particles are wrapped with liposomes and the antibody reduces the saturation magnetization of the immunomagnetic microspheres. Due to the small particle size of CD63-IMB, the magnetic beads may abundantly bind to the cell surface exhibiting a cumulative effect. For this reason, although the saturation magnetization has been reduced to a certain extent, it has no influence on the actual enrichment effects of magnetic separation. The transmission electron microscopy (TEM) and scanning electron microscopy (SEM) results show (Figure 1E,F) that CD63-IMBs are all round shaped with different sizes, with a diameter of about 50 nm, and the distribution is relatively uniform, without obvious agglomeration.

2.2. Exosome Separation and Determination. Under a transmission electron microscope, elliptical membranous particles of the nanometer scale were observed, as shown in Figure 2A. The Brownian motion of exosomes was observed by NTA, as shown in Figure 2B, with an average particle size of 89.78 ± 4.8 nm. The results of Western blot showed that the exosomes of GC cells were rich in exosome markers, CD9 and CD81 (Figure 2C). The fluorescence microscopy imaging analysis showed that marked exosomes were found around the cytoplasm and nucleus of A549 cells (Figure 2D), suggesting that A549 cells could effectively ingest exosomes.

2.3. Results of the qRT-PCR Assay. The qRT-PCR assay is carried out to detect HOTAIR expressions in different lung cancer cell lines, as presented in Figure 3A. Compared with normal human bronchial epithelial cell 16HBE, HOTAIR expressions in lung cancer cell strains NCI-H1395, NCI-H1975, and HCC827 were significantly upregulated, while those in A549 cells were downregulated. In order to verify the effect of exosomes containing HOTAIR on cells with low-expression HOTAIR, exosomes are separated from highly expressed NCI-H1975. By this way, A549 cells with low-expression HOTAIR are treated (Figure 3B). As a result, it is found that HOTAIR expressions are enormously upregulated in A549 cells treated with HOTAIR-containing exosomes.

Similarly, the expression of HOTAIR in lung cancer and normal para-carcinoma tissues is tested using qRT-PCR assays, as shown in Figure 3C. In contrast to normal tissues, HOTAIR is highly expressed in lung cancer tissues. In this case, normal tissues are used as a control to portray ROC curves (see Figure 3D). To be specific, an area under curve (AUC), 95% confidence interval (CI), sensitivity, and specificity are calculated to be 0.723, 0.522−0.924, 74.3, and 77.3%, respectively.

Moreover, qRT-PCR assays are performed to test HOTAIR's expression in serums of both of patients with lung cancer and the healthy control (see Figure 3E). Compared with healthy subjects, the expression of HOTAIR is significantly higher in the serum of lung cancer patients. The ROC curve was drawn with the expression in the serum of healthy subjects as a control. Clearly, AUC, 95% CI, sensitivity, and specificity turn out to be 0.769, 0.597−0.941, 83.3, and 75.0%, respectively (see Figure 3F).

As shown in Figure 3G, qRT-PCR assays are performed to test HOTAIR expressions in exosomes from serums of both of patients with lung cancer and the healthy control. In terms of serums taken from patients with lung cancer, exosomes are enriched with HOTAIR. Compared to the healthy control, it presents a significant increase. HOTAIR expressions in

https://doi.org/10.1021/acsomega.1c00905
ACS Omega 2021, 6, 17217−17227

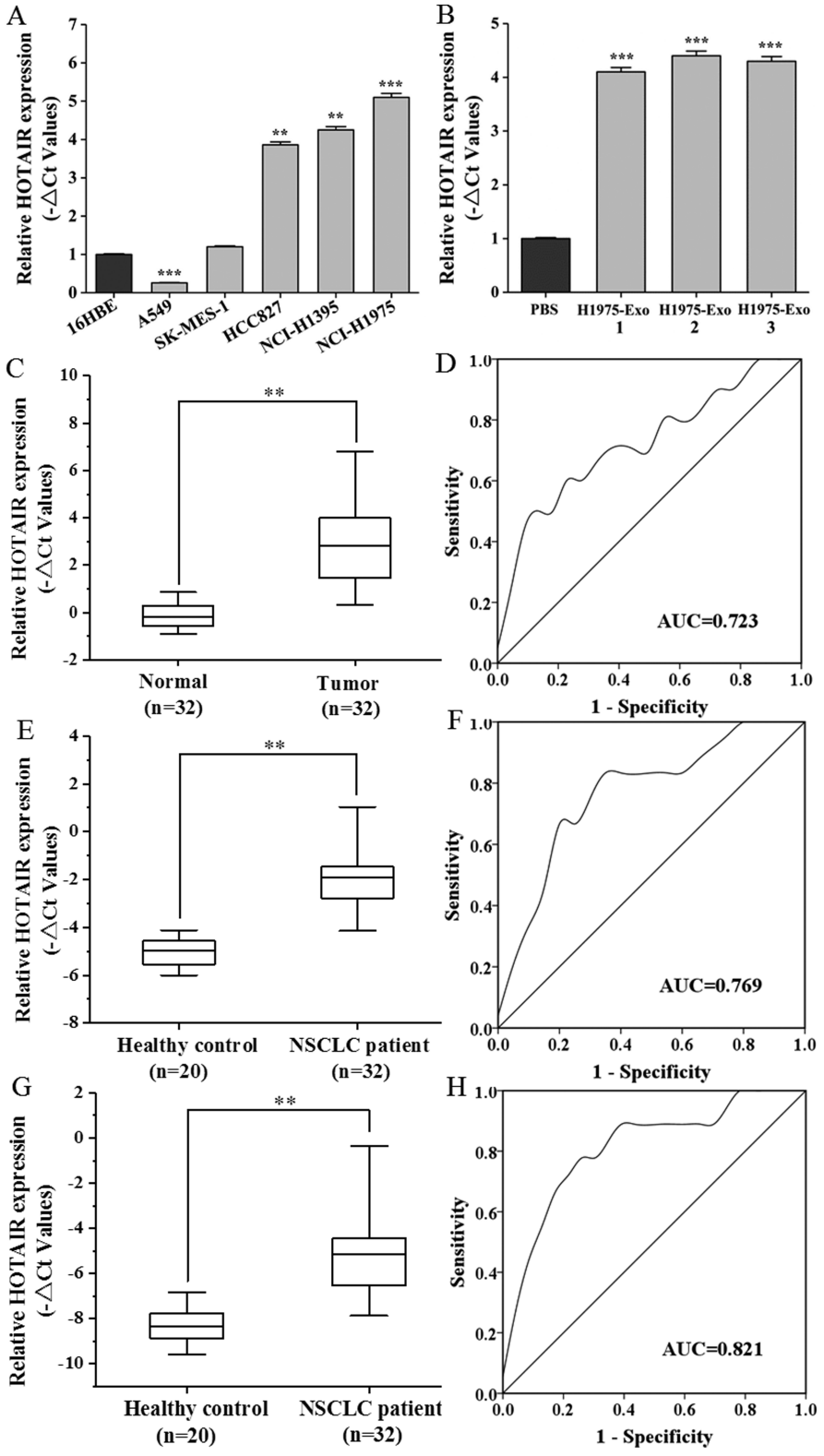

Figure 3. Relative HOTAIR expressions in lung cancer cell lines, tissues, serums, and exosomes isolated from serums. (A) High-expression HOTAIR in NCI-H1975 ($P < 0.001$), but low-expression HOTAIR in A549 cells ($P < 0.001$); (B) relative HOTAIR expressions in A549 cells treated with exosomes derived from NCI-H1975 of 3 patients; (C) relative HOTAIR expressions in lung cancer and normal tissues, where HOTAIR expressions in lung cancer tissues significantly increase highly compared to the normal para-carcinoma tissues; (D) ROC curves of HOTAIR in lung cancer tissues; (E) relative HOTAIR expressions in serums of patients with lung cancer and the healthy control, the expression of HOTAIR in serums of patients with lung cancer show a significant increase compared to the healthy control; (F) ROC curves of FOXM1 in serums of patients with lung cancer; (G) relative HOTAIR expressions in exosomes isolated from serums of patients with lung cancer and the healthy control. HOTAIR expressions in exosomes isolated from serums of patients with lung cancer significantly increase compared to the healthy control; and (H) ROC curves of HOTAIR in exosomes isolated from serums of patients with lung cancer ($*P < 0.05$, $**P < 0.01$, and $***P < 0.001$).

https://doi.org/10.1021/acsomega.1c00905
ACS Omega 2021, 6, 17217−17227

Table 1. Correlation between HOTAIR Expressions ($-\Delta C_t$) in Exosomes Isolated From Serums of Patients with NSCLC and Clinicopathologic Data[a]

features	number of cases (%)	HOTAIR		M ± SD	*P* value	significance
		H	L			
			Sex			
M	22	14	8	−5.24 ± 2.53	0.378	
F	10	5	5	−6.05 ± 1.62		
			Age			
<60	14	9	5	−6.34 ± 1.52	0.573	
≥60	18	11	7	−5.23 ± 2.68		
			Tumor Size (cm)			
<5	17	9	8	−6.24 ± 2.63	0.268	
≥5	15	10	5	−5.98 ± 1.45		
			Differentiation			
moderate	13	8	4	−6.45 ± 2.34	0.534	
poor	19	12	7	−5.74 ± 2.45		
			Lymphatic Metastasis			
None	8	2	6	−6.53 ± 1.63	0.008	**
N1-3	24	19	5	−5.46 ± 2.35		
			Perivenous or Perineuronal Invasion			
Deletion	22	12	10	−6.35 ± 1.76	0.421	
Presence	10	8	2	−5.24 ± 2.36		
			Invasion Depth			
T1 and T2	3	2	1	−4.24 ± 5.10	0.701	
T3 and T4	29	20	9	−6.24 ± 2.35		
			TNM Staging			
I and II	9	3	6	−6.67 ± 2.24	0.012	**
III and IV	23	19	4	−5.85 ± 2.26		

[a]Notes: $P > 0.05$ for insignificant differences; (*) $0.05 < P < 0.01$ for significant differences; and (**) $P < 0.01$ for extremely significant differences.

exosomes of serums from the healthy control are selected as the control. In this context, ROC curves are portrayed, where AUC, 95% CI, sensitivity, and specificity are calculated to be, respectively, 0.821, 0.640−0.983, 88.9, and 78.3% (see Figure 3H). According to the correlation analysis of clinical pathology (see Table 1), HOTAIR expression levels in exosomes isolated from the serums of patients with lung cancer are insignificantly correlated with age, sex, tumor differentiation, or other factors ($P > 0.05$), but associated with lymphatic metastasis ($P = 0.008$) and TNM staging ($P = 0.012$).

2.4. Influence of HOTAIR in Exosomes on Lung Cancer Cell Proliferation and Migration. A549 cells with low-expression HOTAIR are treated with NCI-H1975-derived exosomes containing high-expression HOTAIR. Subsequently, HOTAIR expressions in A549 cells can be tested by means of the qRT-PCR assay, colony formation assay, and flow cytometry (Figure 4). Growth of A549 cells is significantly enhanced after being treated with the exosomes (Figure 4A). According to the results of the colony formation assay, the number of A549 colonies significantly increases (Figure 4B). This manifests that HOTAIR-containing exosomes have the potential to promote lung cancer cell proliferation. According to the qRT-PCR results, cyclin D1 mRNA expression levels go up in A549 cells treated with exosomes, and the results of western blot also reflect that cyclin D1 expressions are upregulated in A549 cells treated with exosomes (Figure 4C). Based on the outcomes of flow cytometry, once A549 cells have been treated with HOTAIR-containing exosomes, the number of cells at the G1 stage declines, while that at the S stage shows a significant increase (Figure 4D). It signifies that exosomes containing HOTAIR can accelerate the progression of the lung cancer cell cycle. According to the apoptosis assay results, expressions of Bcl-2 and Bax in A549 cells treated with exosomes, respectively, increase and decline. Moreover, the Western blot results make it clear that Bcl-2 expressions are upregulated in such cells (Figure 4E), revealing that lung cancer cell apoptosis is suppressed in A549 cells treated with exosomes. As for the Transwell migration assay results concerned, it is clear that for A549 cells treated with HOTAIR-containing exosomes, the number of metastases increased significantly (Figure 4F). Additionally, expression of EMI is also tested by qRT-PCR. The results show decreased E-cadherin expressions, while expressions of N-cadherin, slug, snail, twist, and ZEB1 show an obvious increase (Figure 4G). Western blot experiment is carried out to test EMT-associated gene protein expression, and it is proved that E-cadherin expression is downregulated but N-cadherin, slug, and twist expressions in A549 cells treated with HOTAIR-containing exosomes are upregulated (Figure 4H). Without a doubt, such a result indicates that HOTAIR-containing exosomes have capability to promote lung cancer cell migration. To sum up, it is proved by Transwell migration, qRT-PCR, and Western blot assays that HOTAIR may promote cell migration through induction of EMT.

2.5. Influence of HOTAIR Knockdown on the Proliferation and Migration of Lung Cancer Cells. To further demonstrate the functional roles of HOTAIR in lung cancer, we knocked down HOTAIR expression in lung cancer cells. The results are shown in Figure 5. Growth of NCI-H1975 cells is significantly decreased after being treated with sh-HOTAIR transfected (Figure 5A). According to the results of the colony formation assay, the number of NCI-H1975 colonies significantly declines (Figure 5B). This manifests that sh-HOTAIR-containing exosomes have the potential to inhibit lung cancer cell proliferation. As demonstrated by the qRT-PCR results,

https://doi.org/10.1021/acsomega.1c00905
ACS Omega 2021, 6, 17217−17227

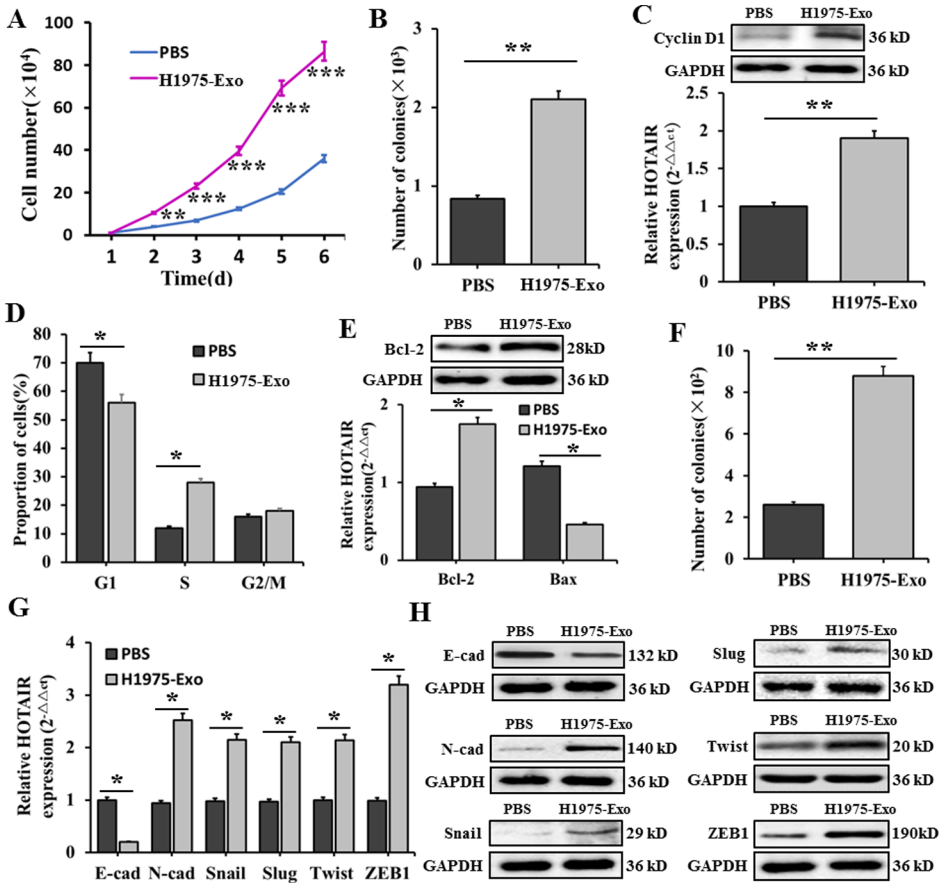

Figure 4. Influence of NCI-H1975-derived exosomal HOTAIR on lung cancer cell proliferation and migration. (A) Growth of A549 cells treated with exosomes according to cell growth curves; (B) Clonality of A549 cells treated with exosomes according to the colony formation assay; (C) Cyclin D1 mRNA and Cyclin D1 protein expressions in A549 cells treated with exosomes according to qRT-PCR and western blot assay; (D) cycle of A549 cells treated with exosomes according to flow cytometry; (E) Bcl-2 protein, Bcl-2, and Bax mRNA expressions in A549 cells treated with exosomes according to qRT-PCR and western blot assay; (F) migration of A549 cells treated with exosomes according to the Transwell migration assay; (G) expressions of EMT-associated mRNA in A549 cells treated with exosomes according to the qRT-PCR assay; and (H) EMT-associated gene protein expressions in A549 cells treated with exosomes according to Western blot.

cyclin D1 mRNA expression levels decreased in NCI-H1975 cells treated with sh-HOTAIR transfected, and the results of western blot also reflect that cyclin D1 expressions are decreased in NCI-H1975 cells treated with sh-HOTAIR transfected (Figure 5C). Based on the outcomes of flow cytometry, once NCI-H1975 cells have been treated with HOTAIR containing sh-HOTAIR transfected, the number of cells at the G1 stage increases, while that at the S stage significantly decreases (Figure 5D). It signifies that HOTAIR depletion could inhibit progression of the lung cancer cell cycle. According to the apoptosis assay results, expressions of Bcl-2 and Bax in NCI-H1975 cells treated with sh-HOTAIR, respectively, decline and increase. Moreover, the Western blot results make it clear that Bcl-2 expressions are decreased in such cells (Figure 5E), revealing that lung cancer cell apoptosis is inhibited in NCI-H1975 cells treated with sh-HOTAIR transfected. As far as the Transwell migration assay results are concerned, it becomes clear that, compared with the control group, the number of migrated NCI-H1975 cells was markedly decreased after sh-HOTAIR transfected treatment (Figure 5F). Additionally, expression levels of EMI-associated mRNA are also tested using the qRT-PCR method. The results show an increase in E-cadherin expressions, while expressions of N-cadherin, slug, snail, twist, and ZEB1 show an obvious increase decreased-(Figure 5G). Western blot experiment is also carried out in order to test EMT-associated gene protein expression levels, proving upregulation of E-cadherin expression but downregulation of N-cadherin, slug, snail, twist, and ZEB1 expressions in NCI-H1975 cells treated with sh-HOTAIR transfected (Figure 5H). Without a doubt, the HOTAIR depletion could inhibit the EMT of lung cancer cells, which led to the suppression of lung cancer cell migration. To sum up, it is proved by Transwell migration, qRT-PCR, and Western blot assays that HOTAIR may promote cell migration through induction of EMT.

3. DISCUSSION

It is reported that inclusions in exosomes may be potential biomarkers for diagnosis and prognosis of lung cancer.[22] Tucci et al. believed that the upregulated PD-1 and CD28 in immune cell derived exosomes may act as predictors of the sensitivity of metastatic melanoma cells to ipilimumab.[23] Furthermore, lncRNA-HEIH expressions are upregulated in exosomes of HCV-associated hepatocellular carcinoma.[24] Relevant studies suggest that exosomes derived from different tumor cells are all enriched with lncRNA. For example, it was found by Yang et al.[25] that ZFAS1 is highly expressed in exosomes isolated from serums of patients with lung cancer; and its expression levels are significantly correlated with lymphatic metastasis and TNM staging. As illustrated by the ROC curves, AUC, 95% CI,

https://doi.org/10.1021/acsomega.1c00905
ACS Omega 2021, 6, 17217−17227

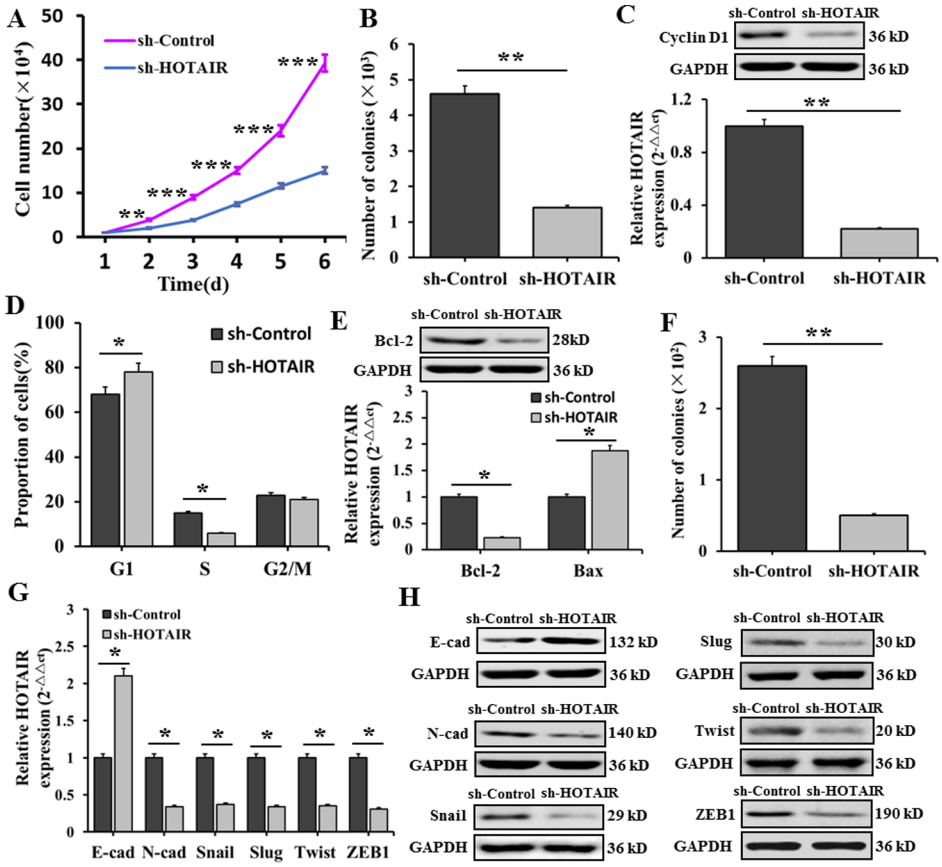

Figure 5. Influence of HOTAIR knockdown on proliferation and migration of lung cancer cells. (A) Growth of NCI-H1975 cells treated with exosomes according to the cell growth curves; (B) clonality of NCI-H1975 cells treated with exosomes according to the colony formation assay; (C) Cyclin D1 mRNA and Cyclin D1 protein expressions in NCI-H1975 cells treated with exosomes according to qRT-PCR and the western blot assay; (D) cycle of NCI-H1975 cells treated with exosomes according to flow cytometry; (E) Bcl-2 protein, Bcl-2, and Bax mRNA expressions in NCI-H1975 cells treated with exosomes according to qRT-PCR and the western blot assay; (F) migration of NCI-H1975 cells treated with exosomes according to the Transwell migration assay; (G) expressions of EMT-associated mRNA in NCI-H1975 cells treated with exosomes according to the qRT-PCR assay; and (H) EMT-associated gene protein expressions in NCI-H1975 cells treated with exosomes according to Western blot.

sensitivity, and specificity reach 0.837, 0.749−0.924, 80.00, and 75.7%, respectively. Therefore, exosomes may promote malignant progression of lung cancer by virtue of ZFAS1 transport. In accordance with the findings of Liu et al.,[26] lncRNA CRNDE-h is highly expressed in exosomes isolated from serums of patients with colon cancer; exosomal CRNDE-h expressions are related to local lymphatic metastasis and distant metastasis of colon cancer; and the cutoff value of serum exosomal CRNDE-h is 0.020, and the corresponding sensitivity and specificity are up to 70.3 and 94.4%, respectively. Based on this, exosomal CRNDE-h is demonstrated to be a noninvasive serum tumor marker for colon cancer diagnosis and prognosis. The above studies prove that exosomal lncRNA may be a potential biomarker for tumors and other diseases. In this study, expressions of lncRNA HOTAIR in exosomes isolated from serums of NSCLC patients are significantly higher than those of healthy people. The HOTAIR expression levels in exosomes have a significant correlation with lymphatic metastasis and the TNM stage. Through analysis of ROC curves, AUC, 95% CI, sensitivity, and specificity of HOTAIR in exosomes are calculated to be, respectively, 0.821, 0.640−0.983, 88.9, and 78.3% as far as NSCLC patients are concerned. Therefore, it was concluded that HOTAIR in exosomes may be a potential biomarker for NSCLC diagnosis, and exosome-derived HOTAIR may provide a new approach to NSCLC diagnosis. Moreover, it provides an experimental basis for our follow-up exploration of the HOTAIR's biological function and mechanism in NSCLC.

In the present study, exosomes isolated from serums of NSCLC patients are proved to contain HOTAIR. Their specific biological functions are still remain unclear. Some studies indicate that HOTAIR plays a critical role in malignant liver neoplasm.[27] In the context where lncRNA HOTAIR expressions in liver cancer tissues are upregulated in a significant way, HOTAIR is believed to promote biological processes, including liver cancer cell proliferation, metabolic reprogramming, and apoptosis.[28] Fang et al. found that HOTAIR regulates HOXA1methylation, further promoting cell apoptosis and cell cycle arrest as well as suppressing tumor growth to enhance the sensitivity of small lung cancer cells to chemotherapeutics.[29] Moreover, overexpressed HOTAIR and chromatin remodeling factor lymphoid-specific helicase are associated with poor prognosis of patients with adenocarcinoma of lung, because they jointly act on FoxA1 and FoxA2, and thus alter their proportions and invasion and migration of tumor cells.[30] It is proved by Wang et al. that HOTAIR's silencing can regulate miR-326, so as to affect Phox2a gene functions, and inhibit proliferation, migration, and tumor growth in cells in nude mice.[31] Zhang et al. found exosomal HOTAIR-promoted proliferation, migration, and invasion through sponging miR-

https://doi.org/10.1021/acsomega.1c00905
ACS Omega 2021, 6, 17217−17227

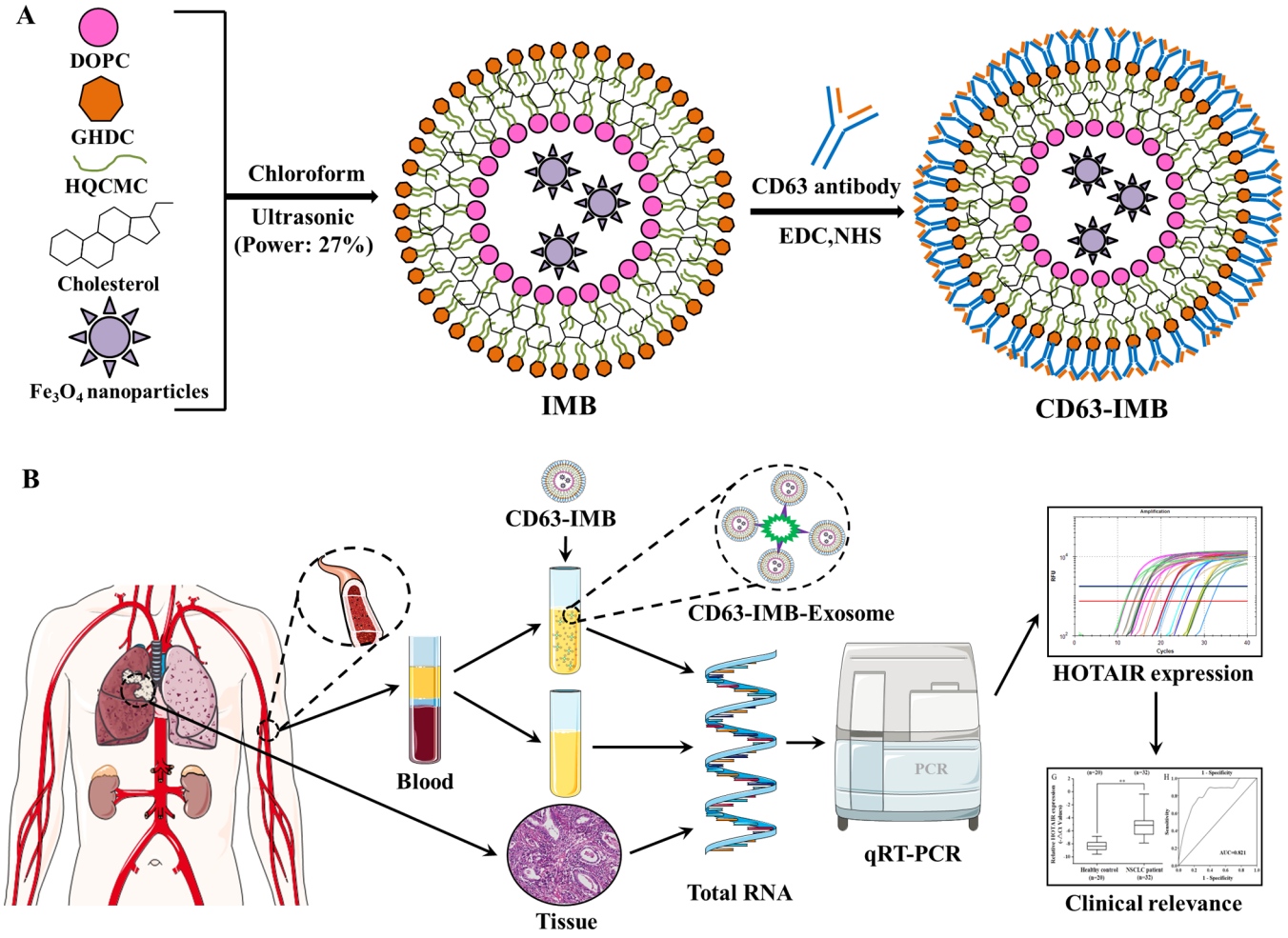

Figure 6. CD63-IMB preparation and flow diagram of the qRT-PCR assay. (A) CD63-IMB preparation flow chart; (B) flow chart of clinical sample testing, and the NSCLC clinical sample detection procedure: tissues and blood of NSCLC patients were collected, and the expression of HOTAIR in tissues, blood, and serum exosomes was detected by qRT-PCR.

203 in lung cancer.[32] Nevertheless, it is still unclear about relations between HOTAIR and exosomes released from lung cancer cells. Purified exosomes derived from NCI-H1975 are utilized to treat A549 cells. Flow cytometry analysis showed that A549 cells can effectively take up exosomes derived from NCI-H1975 cells. After NCI-H1975 exosome treatment, the expression of HOTAIR in A549 cells increased significantly. Additionally, it is revealed by cell growth curves and colony formation assays that proliferation of HOTAIR cells is greatly improved. In line with the Transwell migration assay results, in A549 cells treated with exosomes, not only is migration of HOTAIR cells apparently enhanced, but such a treatment with exosomes has the potential to promote progression of the gastric carcinoma cell cycle and the occurrence of EMT. Furthermore, exosomes derived from gastric carcinoma cells play a role in promoting stomach cancer growth and metastasis with the help of ZFAS1 transport.

Our study found that the expression of HOTAIR in NCI-H1395, NCI-H1975, and HCC827 lung cancer cell strains is significantly higher than that in the normal human bronchial epithelial cell line (16HBE), while its expression decrease in A549 cell strain. Through flow cytometry, it is clear that A549 cells treated with purified NCI-H1975-derived exosomes can uptake exosomes derived from NCI-H1975 cells effectively. Hence, exosomes are isolated from NCI-H1975 cells with high-expression HOTAIR, and then used to treat A549 cells with low-expression HOTAIR. In this way, actions of HOTAIR on lung cancer occurrence and progression can be further investigated. It was found that the expression of HOTAIR in A549 cells was significantly increased after exosome treatment, and that HOTAIR derived from lung cancer cells enhanced the proliferation and migration of lung cancer cells. At the same time, it was found that exosome treatment can promote the cycle progression of gastric cancer cells and the occurrence of EMT. The expression of HOTAIR in A549 cells was significantly increased after exosome treatment, and that HOTAIR derived from lung cancer cells enhanced the proliferation and migration of lung cancer cells. At the same time, exosome treatment can promote the cycle progression of gastric cancer cells and the occurrence of EMT.

4. CONCLUSIONS

In summary, the prepared CD63-IMB can isolate exosomes in serum. The expression of HOTAIR in lung cancer cells, tumor tissues of lung cancer patients, and serum and serum exosomes of lung cancer patients was significantly upregulated. The high expression of HOTAIR in exosomes is significantly related to lymphatic metastasis and TNM staging. Exosomes derived from lung cancer cells can promote the growth and metastasis of lung cancer by transporting HOTAIR. Under the circumstance that

https://doi.org/10.1021/acsomega.1c00905
ACS Omega 2021, 6, 17217−17227

A549 cells are treated with such exosomes, this may promote progression of the stomach cancer cell cycle and the occurrence of EMT. Without a doubt, these results indicate that HOTAIR in exosomes is expected to become a potential biomarker for the diagnosis and treatment of lung cancer, and exosome-derived HOTAIR may provide a new approach to lung cancer treatment.

5. MATERIALS AND METHODS

5.1. Sample Collection and Ethics Statement. 32 NSCLC patients who had received surgical treatment from January 2018 to June 2020 in our hospital were included. According to the clinicopathologic data of all the patients, they had not received any local or systemic treatment before the surgery. The patients' tumor tissues, neighboring non-neoplastic lung tissues, and 15 mL of peripheral blood were sampled. All tissue samples were immediately put into liquid nitrogen for quick freezing and then stored at −80 °C. In addition, 15 mL of peripheral venous blood was taken from 20 healthy volunteers, collected in blood collection tubes containing EDTA anticoagulants, stored, and transported at 4 °C. Moreover, all blood samples taken from healthy subjects should be treated within 72 h. This study has been approved by the Ethics Committee of our hospital, and all patients have signed the informed consent.

5.2. Materials and Instruments. The NSCLC cell lines (i.e., A549, NCI-H1395, NCI-H1975, HCC827, and SK-MES-1) and the normal human bronchial epithelial cell line (16HBE) were purchased from Shanghai cell bank of the Chinese Academy of Sciences; RPMI 1640medium and trypsin were purchased from Gibco company; the ultrapure RNA extraction kit, real-time PCR assay kit, and RNA reverse transcription kit were all purchased from Beyotime Biotechnology; the selected magnetic separation rack was purchased from Huzhou Lieyuan Medical Laboratory; hexadecyl-quaternized (carboxymethyl) chitosans (HQCMC), dimethyl octadecyl epoxypropyl ammonium chloride (GHDC), and 1,2-dioleylphosphatidylcholine (DOPC) were purchased from JuKang (Shanghai) Bio-Sci & Tech Co., Ltd.; N-hydroxysuccinimide (NHS), 1-ethyl 3-(3-dimethylammonium propyl) ammonium bicarbonate (EDC), cholesterol, and other commonly used reagents were purchased from Sinopharm (China); ferroferric oxide (Fe_3O_4) nanoparticles and magnetic separation rack were from Huzhou Lieyuan Medical Laboratory; and the quantitative PCR instrument was purchased from Bio-Rad company in America. At last, ND-1000 NanoDrop was provided by Calibre (Beijing) Technology Development Co., Ltd.

5.3. CD63-IMB Preparation. After HQCMC, Chol, DOPC, GHDC, and Fe_3O_4 nanoparticles were dissolved in chloroform, and an ultrasonic probe was used to carry out ultrasonic oscillation of the mixed solution for 6 min (power: 27%; temperature: 25 °C) at an interval of 1 s; the oscillation continued for 2 s each time. After 30 s of ultrasonic treatment, 6 mL of distilled water was added and then the ultrasonic oscillation proceeded until the solution was completely emulsified. Afterward, rotary evaporation was conducted using a rotary evaporator under conditions of 25 °C, 120 g, and 0.8 Mpa for the purpose of preparing the IMB solution. Then, the prepared IMB solution was mixed with the CD63 antibody at a ratio of 1 mL: 60 μg, coupling agents EDC and NHS were added, and the mixture was oscillated for 24 h at 4 °C. In this way, IMB modified by CD63, named CD63-IMB, was obtained (Figure 6).[33,34]

5.4. CD63-IMB Characterization. 20 μL of the CD63-IMB solution was taken, diluted to 2 mL with ddH_2O. 800 μL of the diluted solution was taken to detect the particle size with a particle size analyzer material RI: 1.59; material absorption: 0.01; dispersant RI: 1.330; viscosity: 0.8872 cP; temperature: 25 °C; duration used: 60 s; and measurement position: 4.65 mm. After that, 50 μL of the diluted solution was further taken and dropped on the mica sheet. With the help of AFM, morphologies of CD63-IMB were observed after drying. Subsequently, 1 mL of it was taken and diluted to carry out UV−vis analysis. 2 mL CD63-IMB solution was taken and lyophilized to detect its magnetic properties by vibrating sample magnetometry. 10 μL of the sample was dissolved in 1 mL of distilled water, 50 μL of the diluted solution was dropped on the copper net, and the shape of the lipid magnetic spheres was observed through a transmission electron microscope. 10 μL of the sample was dissolved in 1 mL of distilled water, 50 μL of the diluted solution was dropped on the sample mirror, and then the shape of the lipid magnetic ball was observed through a scanning electron microscope.

5.5. Exosome Separation and Determination. 7.5 mL of peripheral blood was collected from lung cancer patients and centrifuged for 10 min at 1000*g*. Subsequently, the serum was taken out and put in an EP tube. 20 μL of CD63-IMB was added, incubated for 30 min at room temperature, and mixed once every 5 min. After the incubation, the EP tube was placed on the magnetic separation rack, where separation was carried out for 5 min. Then, the supernatant was sucked out, producing exosomes enriched with CD63-IMB. Furthermore, trypsin (2 mL) was added into the EP tube, a trypsin inhibitor (2 mL) was added after digestion at 37 °C for 10 min, and the tube was vortexed for 5 min and immediately kept in a magnetic separation rack for 10 min. After separation, the supernatant was collected, and thus the exosome suspension was acquired.

10 μL of CD63-IMB rich exosome solution and the exosome solution devoid of CD63-IMB were diluted 100 times with PBS. 800 μL of the diluted solution was taken to detect the particle size with a particle size analyzer. 20 μL of exosome solution was taken and added dropwise in a mesh covered with polyvinyl acetate/carbon for filtering. After preparing the sample, placed it under a transmission electron microscope for observation. In addition, 20 μL exosome solution was taken, the stain Dil was added to this solution, and incubated at 37 °C for 30 min. Three groups of labeled exosome solution were, respectively, added to A549 cells and incubated for 24 h at 37 °C. After completion of the incubation, the culture medium was discarded and the product was wash ed with PBS twice. In the end, imaging analysis was carried out using a fluorescence microscope.

The lysate containing the protease inhibitor PMSF was added to the exosome solution, shaken, mixed, and left to stand on ice for 30 min. Furthermore, a buffer was added to the mixture (1:4) and mixed uniformly as well; and the mixture with buffer was placed in a boiling water bath for 15 min. In addition, 10% sodium dodecyl sulphate-polyacrylamide gel electrophoresis (SDS-PAGE) gel for electrophoresis was prepared; then, electrophoresis was conducted after addition of the gel into protein samples and the marker and eventually tested using an ECL chemiluminescence system.

5.6. RNA Extraction and qRT-PCR. Homogenizing of samples was fulfilled by virtue of TRIzol (Invitrogen, USA). In conformity with instructions on the kit, the total RNA was extracted. After quantification by NanoDrop 2000 (Thermo Fisher Scientific Inc., USA), 200 ng total RNAs were reversely transcribed according to directions of the ReverTra Ace qPCR RT Kit (Toyobo, Japan). Then, qRT-PCR analysis was carried

https://doi.org/10.1021/acsomega.1c00905
ACS Omega 2021, 6, 17217−17227

out on the resulting product of reverse transcription by THUNDERBIRD SYBR qPCR Mix (Toyobo, Japan). Moreover, qRT-PCR was completed by virtue of a CFX96 Touch Real-Time PCR Detection System (Bio-Rad). In order to determine the mRNA content, GAPDH was selected as the internal control. Four primers used for HOTAIR were 5′-CAGTGGGGAACTCTGACTCG-3′ (forward), 5′-GTGCCTGGTGCTCTCTTACC-3′ (reverse), GAPDH forward 5′-GGGAGCCAAAAGGGTCAT-3′, and GAPDH reverse 5′-GAGTCCTTCCACGATACCAA-3′. At last, the corresponding results were analyzed by means of a $2^{-\Delta\Delta C_t}$ method applicable to relative quantification.

5.7. Gene Silencing. The sh-HOTAIR directed against silencing HOTAIR plasmid was purchased from General biosystems (Anhui) Co., Ltd. The sequence of sh-HOTAIR was (5′-AAAUCCAGAACCCUCUGACAUUUGC-3′). NCI-H1975 cells were grown in 6-well plates (2×10^6/well) and transfected for 36 h using the HB-TRLF-1000 LipoFiter transfection reagent.

5.8. Cellular Intervention. 10% FBS was ultracentrifuged for 12 h at $1 \times 10^5 g$ for 12 h to remove the exosome. The culture medium with exosome removed was used to incubate NCI-H1975 cells. In addition, NCI-H1975-derived exosomes (100 μg/mL) and PBS were, respectively, added to A549 cells.

5.9. Cell Growth Curve Determination. The LipoFiter lipofection transfection reagent was selected to perform cell transfection for 36 h. Moreover, the cells were digested by trypsin into single-cell suspension, and then incubated in a 24-well plate (concentration: 1×10^4 cells each well). Cell counting was made every 24 h for six consecutive days. Then, time and the cell count were, respectively, used as horizontal and vertical coordinates. In this way, a cell growth curve could be portrayed. Additionally, the experiment was performed in triplicate per well.

5.10. Colony Formation Assay. Transfected cells were digested by trypsin into single-cell suspension that was further incubated on a 6-well plate (concentration: 1×10^3 cells each well) at constant temperature (i.e., 37 °C). The culture medium was changed every three days. 10 days later, the cell clone status was observed. The culture supernatant was removed and washed twice with PBS and then fixed by 4% paraformaldehyde fixative for 30 min. After staining with crystal violet for 15 min, the cells were washed twice with PBS. Moreover, the experiment was also performed in triplicate for each well. Finally, they were placed under a microscope for photographing and cell counting.

5.11. Transwell Migration Assay. Trypsin was utilized to digest transfected cells into a single-cell suspension. After that, the cells were incubated in a serum-free medium and then placed in an upper chamber of a Transwell plate. Moreover, its lower chamber had a medium containing 10% FBS. In this manner, the cells were cultured in an incubator for 36 h at constant temperature (i.e., 37 °C). After that, the chamber was taken out and sucked up the upper chamber fluid. Cells not migrated from the surface of the inner membrane in the cabin were gently wiped off by using swabs. Subsequently, the cabin was put in 4% paraformaldehyde fixative solution to fix the cells for 30 min and stained with crystal violet for 15 min, and the cells were rinsed with PBS three times. Moreover, the experiment was performed in triplicate for each well. Finally, the plate was dried in the air and placed under a microscope for photographing and cell counting.

5.12. Cell Cycle Determination. Transfected cells in the logarithmic growth phase were digested by trypsin into single-cell suspension, precooled using absolute ethyl alcohol, mixed by pipetting, fixed overnight at 4 °C, and then centrifuged for 10 min at 800 g. Subsequently, the cells added with RNase A were kept in a water bath for 30 min at 37 °C; then, they were stained with propidium iodide (PI) of 100 μg/mL in a dark place at room temperature. At last, cells in different cell cycles were counted on a flow cytometer.

5.13. Cell Apoptosis Assay. The prepared single-cell suspension was centrifuged at 4 °C and 800 rpm for 10 min. 1× Binding buffer was prepared (4 mL binding buffer + 12 mL deionized water) and added into the PBS for cell resuspension. In this case, the concentration was adjusted to 1×10^6/mL and 100 μL cells were suspended in a 5 mL flow tube. Successively, 5 μL Annexin Alexa Fluor 647 and 10 μL PI were added. The tube was gently shaken to blend them uniformly. Then, the mixture was kept in a dark place for 15 min at room temperature. Furthermore, 400 μL of the PBS was added to uniformly mix with cells and other solutions there. At last, cell apoptosis was carried out using a flow cytometer in 1 h.

5.14. Western Blot. RIPA lysis buffer was added into the samples. After homogenization, pyrolysis, and centrifugation, the total protein extract was obtained. By means of the Bradford assay, the protein concentration in the extract could be determined, subsequent to SDS-PAGE for proteins. Similarly, the chemiluminescent solution was added after the membrane was rinsed, which was followed by squash, exposure, and photographic fixing. The software Lab Works 4.5 was used for image acquisition, analysis, and determining integrated optical density of protein bands. In addition, the GAPDH protein band of each sample was tested as the internal control.

5.15. Statistical Analysis. Data analysis and statistical mapping were, respectively, carried out by SPSS 21.0 and GraphPad Prism 6.0. Measurement data are expressed in mean ± standard deviation (M ± SD); *T*-test or variance analysis (ANOVA) is selected for intergroup comparison of these data conforming to the normal distribution. Regarding the remaining measurement data failing to be consistent with the normal distribution, the Wilcoxon rank-sum test is adopted. In terms of the enumeration data, the χ-square test is applied. $P < 0.05$ indicates that differences in these data are of statistical significance.

AUTHOR INFORMATION

Corresponding Author

Qihong Zhuang − *Department of Pulmonary and Critical Care Medicine, The First Affiliated Hospital of Xiamen University, Xiamen City, Fujian Province 361001, China;* orcid.org/0000-0002-3295-2669; Email: zhuangqihong1@163.com

Authors

Lanlan Chen − *Department of Pulmonary and Critical Care Medicine, The First Affiliated Hospital of Xiamen University, Xiamen City, Fujian Province 361001, China*

Shenhui Huang − *Department of Pulmonary and Critical Care Medicine, The First Affiliated Hospital of Xiamen University, Xiamen City, Fujian Province 361001, China*

Jincheng Huang − *Department of Pulmonary and Critical Care Medicine, The First Affiliated Hospital of Xiamen University, Xiamen City, Fujian Province 361001, China*

Qiujuan Chen − *Department of Pulmonary and Critical Care Medicine, The First Affiliated Hospital of Xiamen University, Xiamen City, Fujian Province 361001, China*

Complete contact information is available at:

https://doi.org/10.1021/acsomega.1c00905
ACS Omega 2021, 6, 17217−17227

https://pubs.acs.org/10.1021/acsomega.1c00905

Notes

The authors declare no competing financial interest.

REFERENCES

(1) Miranda-Filho, A.; Bray, F.; Charvat, H.; Rajaraman, S.; Soerjomataram, I. The world cancer patient population (WCPP): An updated standard for international comparisons of population-based survival. *Cancer Epidemiol.* **2020**, *69*, 101802−101805.

(2) Zang, J.; Hu, Y.; Xu, X.; Ni, J.; Yan, D.; Liu, S.; He, J.; Xue, J.; Wu, J.; Feng, J. Elevated serum levels of vascular endothelial growth factor predict a poor prognosis of platinum-based chemotherapy in non-small cell lung cancer. *OncoTargets Ther.* **2017**, *10*, 409−415.

(3) Fei, M.; Luo, Y.; Zhou, J.; Yan, Q. The role of Livin expression in the clinicopathological features and prognosis of lung cancer: a meta-analysis. *Transl. Cancer Res.* **2021**, *10*, 99−109.

(4) Erkmen, C. P.; Dako, F.; Moore, R.; Dass, C.; Ma, G. X. Adherence to annual lung cancer screening with low-dose CT scan in a diverse population. *Canc. Causes Contr.* **2021**, *1*, 291.

(5) Minamiya, Y.; Saito, H.; Ito, M.; Imai, K.; Konno, H.; Takahashi, N.; Motoyama, S.; Ogawa, J.-i. Suppression of Zinc Finger Homeobox 3 expression in tumor cells decreases the survival rate among non-small cell lung cancer patients. *Cancer Biomarkers* **2012**, *11*, 139−146.

(6) Zehentmayr, F.; Grambozov, B.; Kaiser, J.; Fastner, G.; Sedlmayer, F. Radiation dose escalation with modified fractionation schedules for locally advanced NSCLC: A systematic review. *Thorac. Cancer* **2020**, *11*, 1375−1385.

(7) Li, X.; Zhang, D.; Li, B.; Zou, B.; Wang, S.; Fan, B.; Li, W.; Yu, J.; Wang, L. Clinical implications of germline BCL2L11 deletion polymorphism in pretreated advanced NSCLC patients with osimertinib therapy. *Lung Cancer* **2021**, *151*, 39−43.

(8) Qi, Y.; Yang, W.; Liu, S.; Han, F.; Wang, H.; Zhao, Y.; Zhou, Y.; Zhou, D. Cisplatin loaded multiwalled carbon nanotubes reverse drug resistance in NSCLC by inhibiting EMT. *Canc. Cell Int.* **2021**, *21*, 74.

(9) Zhang, C. G.; Yin, D. D.; Sun, S. Y.; Han, L. The use of lncRNA analysis for stratification management of prognostic risk in patients with NSCLC. *Eur. Rev. Med. Pharmacol. Sci.* **2017**, *21*, 115−119.

(10) Zhang, B.; Haiji, W.; Jinpeng, P.; Jiang, W. Knockout of lncRNA UCA1 inhibits drug resistance to gefitinib via targeting STAT3 signaling in NSCLC. *Minerva Med.* **2019**, *110*, 273−275.

(11) Loewen, G.; Jayawickramarajah, J.; Zhuo, Y.; Shan, B. Functions of lncRNA HOTAIR in lung cancer. *J. Hematol.* **2014**, *7*, 90−99.

(12) Gupta, R. A.; Shah, N.; Wang, K. C.; Kim, J.; Wong, D. J.; Tsai, M.-C.; Hung, T.; Argani, P.; Rinn, J. L.; Wang, Y.; Brzoska, P.; Kong, B.; Li, R.; West, R. B.; van de Vijver, M. J.; Sukumar, S.; Chang, H. Y. Long non-coding RNA HOTAIR reprograms chromatin state to promote cancer metastasis. *Nature* **2010**, *464*, 1071−1076.

(13) Bhan, A.; Mandal, S. S. LncRNA, HOTAIR A master regulator of chromatin dynamics and cancer. *Biochim. Biophys. Acta, Rev. Cancer* **2015**, *1856*, 151−164.

(14) Ishibashi, M. Clinical significance of the expression of long non-coding RNA HOTAIR in primary hepatocellular carcinoma. *Oncol. Rep.* **2013**, *29*, 946−950.

(15) Wu, J.; Tang, Q.; Ren, X.; Zheng, F.; Chai, X. Reciprocal interaction of HOTAIR and SP1 together enhance the ability of Xiaoji decoction and gefitinib to inhibit EP4 expression. *J. Ethnopharmacol.* **2019**, *237*, 128−140.

(16) Zhang, X.; Xiao, Y.; Hui, S.; Wu, L.; Hui, Q.; Xu, W. Exosomes in cancer: small particle, big player. *J. Hematol. Oncol.* **2015**, *8*, 83.

(17) Yang, H.; Fu, H.; Xu, W.; Zhang, X. Exosomal non-coding RNAs: a promising cancer biomarker. *Clin. Chem. Lab. Med.* **2016**, *54*, 1871−1879.

(18) Fang, J. H.; Zhang, Z. J.; Shang, L. R.; Luo, Y. W.; Lin, Y. F.; Yuan, Y.; Zhuang, S. M. Hepatoma cell-secreted exosomal microRNA-103 increases vascular permeability and promotes metastasis by targeting junction proteins. *Hepatology* **2018**, *68*, 1459−1475.

(19) Li, Y.; Zheng, Q.; Bao, C.; Li, S.; Guo, W.; Zhao, J.; Chen, D.; Gu, J.; He, X.; Huang, S. Circular RNA is enriched and stable in exosomes: a promising biomarker for cancer diagnosis. *Cell Res.* **2015**, *25*, 981−984.

(20) Li, Q.; Shao, Y.; Zhang, X.; Zheng, T.; Miao, M.; Qin, L.; Wang, B.; Ye, G.; Xiao, B.; Guo, J. Plasma long noncoding RNA protected by exosomes as a potential stable biomarker for gastric cancer. *Tumor Biol.* **2014**, *36*, 2007−2012.

(21) Dong, L.; Lin, W.; Xiaoben, Z.; Dong, X.; Lei, S.; Weiqi, L. Circulating Long RNAs in Serum Extracellular Vesicles: Their Characterization and Potential Application as Biomarkers for Diagnosis of Colorectal Cancer. *Cancer Epidemiol.* **2016**, *25*, 1158−1166.

(22) Salehi, M.; Sharifi, M. Exosomal miRNAs as novel cancer biomarkers: Challenges and opportunities. *J. Cell. Physiol.* **2018**, *233*, 6370−6380.

(23) Tucci, M.; Passarelli, A.; Mannavola, F.; Stucci, L. S.; Ascierto, P. A.; Capone, M.; Madonna, G.; Lopalco, P.; Silvestris, F. Serum exosomes as predictors of clinical response to ipilimumab in metastatic melanoma. *Oncoimmunology* **2018**, *7*, No. e1387706.

(24) Zhang, C.; Yang, X.; Qi, Q.; Gao, Y.; Wei, Q.; Han, S. lncRNA-HEIH in serum and exosomes as a potential biomarker in the HCV-related hepatocellular carcinoma. *Canc. Biomarkers* **2018**, *21*, 651−659.

(25) Yang, H.; Fu, H.; Xu, W.; Zhang, X. Exosomal non-coding RNAs: a promising cancer biomarker. *Clin. Chem. Lab. Med.* **2016**, *54*, 1871−1879.

(26) Liu, T.; Zhang, X.; Gao, S.; Jing, F.; Yang, Y.; Du, L.; Zheng, G.; Li, P.; Li, C.; Wang, C. Exosomal long noncoding RNA CRNDE-h as a novel serum-based biomarker for diagnosis and prognosis of colorectal cancer. *Oncotarget* **2016**, *7*, 85551−85563.

(27) Yang, L.; Zhang, X.; Li, H.; Liu, J. The long noncoding RNA HOTAIR activates autophagy by upregulating ATG3 and ATG7 in hepatocellular carcinoma. *Mol. Biosyst.* **2016**, *12*, 2605−2612.

(28) Cai, B.; Song, X. Q.; Cai, J. P.; Zhang, S. HOTAIR: a cancer-elated long non-coding RNA. *Neoplasma* **2014**, *61*, 379.

(29) Fang, S.; Gao, H.; Tong, Y.; Yang, J.; Tang, R.; Niu, Y.; Li, M.; Guo, L. Long noncoding RNA-HOTAIR affects chemoresistance by regulating HOXA1 methylation in small cell lung cancer cells. *Lab. Invest.* **2016**, *96*, 60−68.

(30) Wang, R.; Shi, Y.; Chen, L.; Jiang, Y.; Mao, C.; Yan, B.; Liu, S.; Shan, B.; Tao, Y.; Wang, X. The ratio of FoxA1 to FoxA2 in lung adenocarcinoma is regulated by LncRNA HOTAIR and chromatin remodeling factor LSH. *Sci. Rep.* **2015**, *5*, 17826−17836.

(31) Wang, R.; Chen, X.; Xu, T.; Xia, R.; Han, L.; Chen, W.; De, W.; Shu, Y. MiR-326 regulates cell proliferation and migration in lung cancer by targeting phox2a and is regulated by HOTAIR. *Am. J. Cancer Res.* **2016**, *6*, 173.

(32) Zhang, C.; Xu, L.; Deng, G.; Ding, Y.; Bi, K.; Jin, H.; Shu, J.; Yang, J.; Deng, H.; Wang, Z.; Wang, Y. Exosomal HOTAIR promotes proliferation, migration and invasion of lung cancer by sponging miR-203. *Sci. China: Life Sci.* **2020**, *63*, 1265−1268.

(33) Ding, J.; Wang, K.; Tang, W.-J.; Li, D.; Wei, Y.-Z.; Lu, Y.; Li, Z.-H.; Liang, X.-F. Construction of Epidermal Growth Factor Receptor Peptide Magnetic Nanovesicles with Lipid Bilayers for Enhanced Capture of Liver Cancer circμLating tumor cell. *Anal. Chem.* **2016**, *88*, 8997−9003.

(34) Liang, X.; Shi, B.; Wang, K.; Fan, M.; Jiao, D.; Ao, J.; Song, N.; Wang, C.; Gu, J.; Li, Z. Development of self-assembling peptide nanovesicle with bilayers for enhanced EGFR-targeted drug and gene delivery. *Biomaterials* **2016**, *82*, 194−207.

https://doi.org/10.1021/acsomega.1c00905
ACS Omega 2021, 6, 17217−17227